


RESEARCH

Open Access



Paint has the potential to release microplastics, nanoplastics, inorganic nanoparticles, and hybrid materials

Cheng Fang^{1,2*} , Wenhao Zhou³, Jiaqi Hu³, Cuiqin Wu⁴, Junfeng Niu⁵ and Ravi Naidu^{1,2}

Abstract

Background When we paint our houses or offices, we might paint plastic, because most paints are generally formulated with polymer binders. After drying and curing, the binders fix the colourants on the painted surface as a film of plastic mixture, which is tested herein using Raman imaging to analyse and directly visualise the hybrid plastic-colourant (titanium dioxide or TiO₂ nanoparticles).

Results For the plastic mixture or hybrid, the co-existence and competition between the Raman signals of plastic and TiO₂ complicate the individual analysis, which should be carefully extracted and separated in order to avoid the weak signal of plastic to be masked by that of TiO₂. This is particularly important when considering the Raman activity of TiO₂ is much stronger than that of plastic. Plastic is observed to coat the TiO₂ nanoparticle surface, individually or as a bulk to embed the TiO₂ nanoparticles as mixture or hybrid. Once branched, pended, scratched or aged, the paint can also be peeled off from the painted surface, including gyprock, wood and glass, releasing microplastics and nanoplastics (coating onto the individual TiO₂ nanoparticle surface or embedding the TiO₂ nanoparticles, or individually as particles) in potential.

Conclusions Our test sends us a warning that we are surrounded by plastic items that might release microplastics and nanoplastics in potential, for which the risk assessment is needed. Overall, Raman imaging is a suitable approach to effectively characterise microplastics and nanoplastics, even from the mixture with the hybrid background and the complicated interference.

Keywords Paint, Plastic binder, Raman imaging, Microplastics, Nanoplastics, TiO₂ nanoparticle

*Correspondence:

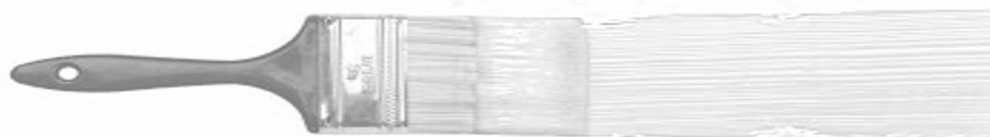
Cheng Fang
cheng.fang@newcastle.edu.au

Full list of author information is available at the end of the article

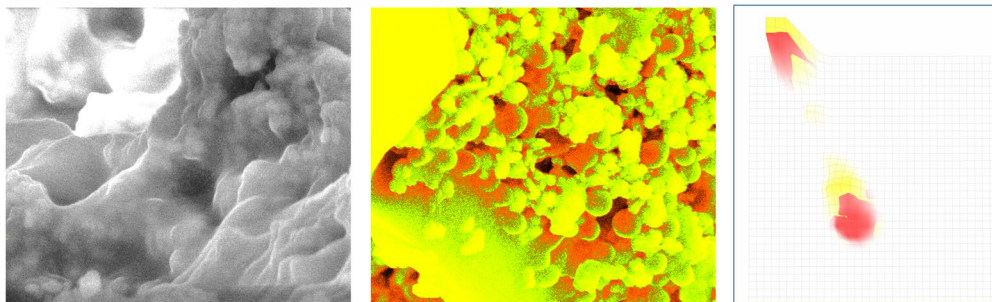


© The Author(s) 2024. **Open Access** This article is licensed under a Creative Commons Attribution 4.0 International License, which permits use, sharing, adaptation, distribution and reproduction in any medium or format, as long as you give appropriate credit to the original author(s) and the source, provide a link to the Creative Commons licence, and indicate if changes were made. The images or other third party material in this article are included in the article's Creative Commons licence, unless indicated otherwise in a credit line to the material. If material is not included in the article's Creative Commons licence and your intended use is not permitted by statutory regulation or exceeds the permitted use, you will need to obtain permission directly from the copyright holder. To view a copy of this licence, visit <http://creativecommons.org/licenses/by/4.0/>.

Graphical Abstract



Micro- / nanoplastic / TiO₂ nanoparticle hybrids in paint



Background

The global paint and coating market was valued at USD~160 billion in 2021 and predicted to grow to USD~235 billion by 2029 [1]. In paint, typical components include colourant/pigment, solvent, binder and additives [2, 3, 4]. Among them, binder is the key component because it provides the film-forming properties of the paint for holding the colourants and other components together, and generates adhesion to the to-be-painted surface [5]. Most of binders are made of polymers, including acrylic, vinyl, polyester, etc. In this case, these paints can be categorised as plastic-based ones, to be differentiated from others [6]. Unfortunately, the widespread use of plastic-based paints has contributed to the environment contamination [7], particularly these paint-film materials can break down into small particles and fragments that are emerging contaminants of microplastics (<5 mm) and even nanoplastics (<1000 nm) [8]. Given our houses and offices are usually painted and we are daily exposed to the paints, the study and characterisation of paints are urgently needed, from the microplastic perspective [9].

Microplastic is a growing concern for the environment and the public health due to the widespread presence in various ecosystems [9, 10]. Microplastics can enter our food chain through ingestion by marine organisms, potentially causing harm to both marine lives and humans [11]. More seriously, we might have been exposed to microplastics and even nanoplastics from our

daily lives that we have not yet paid much attention, such as paint around us that can potentially release debris of microplastics and nanoplastics [9, 12, 13], which is studied herein.

Unfortunately, characterising microplastics is a challenge due to the small size, irregular shape, and diverse composition [10]. Microplastics can come in a variety of forms, including fibres, fragments, particles and pellets, and can be made from different types of polymers [9, 14, 15]. Additionally, microplastics can absorb other pollutants, making it difficult to determine their original compositions, particularly after weathering and ageing. Beyond the pure plastics, the plastic mixture such paint has many components originally. Each component has its own signal that can interfere with the plastic detection [6], which further complicates the plastic characterisation. Microplastics are often detected using specialised analytical techniques, such as infrared spectroscopy (IR) or Raman spectroscopy, which can identify the chemical components from molecular spectrum perspective [10, 16]. Raman is becoming a popular technique for the microplastics characterisation, owing to the no interference from water and the laser-based approach, which even enables the detection of nanoplastics [17]. However, the weak Raman signal of plastics might lead to the false positive/negative results. This is particularly challenging once its Raman activity is weaker than the co-existent component that can easily mask and shield the analysis of plastics, such as in paint.

Raman imaging is a powerful analytical technique that can be used to identify and characterise the microplastics and nanoplastics [10]. By scanning the laser on the sample surface, the molecular spectrum can be collected along with the physical position information to generate a hyper spectrum matrix. The matrix is analysed to generate image to directly visualise the microplastics and nanoplastics from a chemical window or channel, using their specific Raman spectra towards mapping [18, 19]. The hyperspectral matrix collected from the scanning (not a single spectrum from only a position) can enhance the signal, from statistical point of view [20–23]. However, it also presents certain new challenges. One of the main challenges in using Raman imaging for the plastic characterisation is the potential interference from other co-components such as in paint, as mentioned. Secondly, the small size of microplastics particularly nanoplastics makes it difficult to obtain accurate Raman signal due to the limited amount of material available for analysis. Thirdly, the conversion from the hyperspectral matrix to image is a tough job and chemometrics are usually needed [24–26].

This report studies the micro-/nanoplastics released from our house/office paints through several pathways, including droplet, paint branch/boundary, surface run-off and degradation of paint over time. By advancing the Raman imaging to overcome the characterisation challenges, the plastic components in the paint mixture can be well extracted towards visualisation. The hybrid/mixture structure of plastic-coating nanoparticles or plastic-embedding-nanoparticle are identified to be different from the pure plastics. This research on micro-/nanoplastics in house/office paints can help to raise public awareness of the issue and promote consumer choices. Overall, research on microplastics in house/office paint is critical to address the growing concern on micro-/nanoplastic contamination and to develop effective plastic characterisation to protect the environment and human health.

Methods

Chemicals and samples

All chemicals including ethanol and acetone were purchased from Sigma-Aldrich (Australia) and used as received. Milli Q water (>18 M Ω cm) was used for the analysis.

The virgin microplastic powders or pellets of polystyrene (PS), polyethylene terephthalate (PET), polyethylene (PE), polyvinyl chloride (PVC) and polypropylene (PP) were purchased from Sigma-Aldrich (Australia) and used as received. Several Raman spectra were extracted from the database when the standard plastic samples were not available, such as from Dong et al.

[27] or from Rochman Lab, including polyamide (PA or PA 6), poly(methyl methacrylate) (PMMA), polycarbonate (PC), polyurethane (PUR) and acrylonitrile butadiene styrene (ABS). As emphasised by Rochman Lab, these spectra might be not collected from the pure plastic samples and some interferences can be mixed with the plastic signal.

There are many types of paint on the market and the components vary significantly [8], as shown in Additional file 1: Figure S1. We purchased 4 paint samples (#1–#4) from a local market (Bunnings Warehouse, NSW, Australia), as presented in Additional file 1: Figure S1.

For sample preparation, the paint was homogenised for at least 5 min by shaking, as suggested by the paint introduction. Then using a brush or roller, the paint was distributed onto the surface of glass, wood or gyprock (all surfaces have been cleaned in advance, using tap water and common paper tissues), as demonstrated in Additional file 1: Figure S1. Once the solvent (water or oil) evaporates, with the help of additives, the binder forms a plastic film to fix the colourant (such as titanium dioxide, TiO₂) onto the painted surface with different colour.

From this cured paint (such as after one day of evaporation) and the peeled-off paint film shown in Additional file 1: Figure S1, we also tried to chemically remove TiO₂ using the concentrated nitric acid and hydrogen chloride acid for incubation overnight, in order to dissolve it but failed. The TiO₂ was so stable (or protected by the plastic film) to resist the acids for reaction, only slightly yellowed surface (plastics is proposed to be reacted) was observed. From Raman results, the signal of TiO₂ is not disappeared but even strengthened to some degree, while the plastic signal weakened.

We also tried to separate the different components in the paint for test. In this case, we took ~10 mL paint (such as Sample #1) into a ~15 mL centrifuge tube, as shown in Additional file 1: Figure S1. After centrifuge for ~30 min at 4,700 revolutions per minute (rpm), the top layer (mainly solvent) was removed. The bottom layer (colourant of TiO₂) was washed with Milli Q water, ethanol and acetone with help of sonication, respectively. Regarding the middle layer, ~1 mL was transferred to ~2 mL centrifuge tube and worked at 12,000 rpm for another ~30 min. The different layers of binder (in total of 4 middle layers) in the tube were samples and tested. Another option for the separation is to employ the coffee-ring capillary force to work like a chromatography [28]. In this case, a droplet (~0.1 mL) of the middle layer was mixed with a similar amount of ethanol, dropped onto the glass surface (previously cleaned with tap water, Milli Q water, ethanol), and dried in air as a coffee-ring. Within the coffee-ring, from central to boundary, the four-layer/ring can be observed for test as well.

During the painting process, the paint droplets are observed in Additional file 1: Figure S1, which can be categorised as microplastics and nanoplastics, if the plastic component can be confirmed from the mixture or hybrid, as studied herein.

After the painting, the ageing, weathering and degradation of paints can release debris that might be microplastics and nanoplastics too. In this case, we also collected paint samples (#5–#9) from house and office where the paints have been applied for ~5–20 years. The trade/brand information is thus not available, and the samples are shown in Additional file 1: Figure S1.

Raman test

Raman spectra were recorded in air using a confocal Raman microscope (Alpha 300RS, Germany; or DXRxi/ThermoFisher, USA) equipped with 532 nm laser diode (<30 mW) [29]. In general, a charge-coupled device (CCD) detector was cooled at $-60\text{ }^{\circ}\text{C}$ to collect Stokes Raman signals under an objective lens (100 \times , or others such as 40 \times , 20 \times) at room temperature ($\sim 24\text{ }^{\circ}\text{C}$).

To map the image, the laser was scanning on the sample surface to excite the Raman scattering. Simultaneously, the Raman signal was collected at each pixel or physical position as a hyper-spectrum. The pixel size, such as at $0.33\text{ }\mu\text{m}\times 0.33\text{ }\mu\text{m}$, can be adjusted by selecting the scanning area (e.g. $10\text{ }\mu\text{m}\times 10\text{ }\mu\text{m}$) and controlling the scanning pixel array (e.g. 30×30). The integration time at each pixel was 1 s or others, which was adjustable as well and listed in Additional file 1: Table S1.

The collected Raman signal was analysed using WITec Project software to map the characteristic peak of plastic at the pixel array as an image. The peak background (spectrum) has been generally subtracted using the collected signal at both sides of the selected characteristic Raman peak at each pixel as the spectrum background, if no further indication. To further avoid the “bias and false” imaging, an imaging-algorithm analysis is recommended, as discussed below.

Logic-based algorithm for image merge

From the Raman spectra matrix, several images can be simultaneously mapped from the same spectrum at several different characteristic peaks. Corresponding to two or more different characteristic peaks, two or more images can be mapped and subsequently merged, such as by logic-OR, or colour-channel-merge, using ImageJ software. In the latter case to use colour-channel-merge, the original colour can be maintained to distinguish their contributions individually.

In the case of “logic-OR”, any mapped signal (or dot, pixel) from any image (two or more parent images) will be picked up and merged into a new image (daughter

image). Obviously, any “bias and false” noise from any parent images (mapped at two or more different Raman peaks) might be picked up and appear in the daughter image. We thus should balance between the signal merging and the noise pickup.

Correlation analysis for plastic identification

To identify the plastic, the collected Raman spectrum is combined with standard spectrum library to digitally compare them via correlation, akin to indexing [30]. In this case, the sample Raman spectrum was mixed with 10 common plastics including PS, PET, PE, PVC, PP, PA, PMMA, PC, PUR, and ABS. The mixture data of the Raman spectrum were analysed by principal component analysis (PCA) with help of software OriginPro (2023), as reported before [31]. The generated correlation matrix enables the assignment of the suspected items, automatically and digitally.

SEM

An SEM (Zeiss Sigma VP) equipped with a backscattered electron detector (BSD) was used to characterise the morphology of the micro-/nanoplastics, in addition to energy-dispersive X-ray spectroscopy (EDS) detection. The painted glass, wood and gyprock were cut using strong scissors to small pieces of $< \sim 1\text{ cm}\times 1\text{ cm}$, and stucked onto the SEM holder using carbon tape. The peeled-off samples (paint films) were directly deposited onto the carbon tape surface. Before loading into the SEM chamber, the samples were sputter-coated with a thin layer of platinum ($\sim 10\text{ nm}$) to increase the conductivity. The wood and gyprock samples should be pre-treated in an oven at $\sim 60\text{ }^{\circ}\text{C}$ overnight to dry off the water moisture, to get ready for the subsequent vacuum working conditions.

Results and discussion

SEM

The general paint looks like a bulk film, as shown in Fig. 1a, collected from the painted glass surface. Once zoomed in, image (b) shows the particles, some of which are not yet completely bonded together by the binder. The different brightness (white vs. grey) means different conductivity that might originate from the different degree/amount of painted polymer on the surface. That is, the particles are “painted”, shelled and coated by the binder polymer, individually or as a bulk. These particles of spheres with diameters in the range of 300–500 nm are colourant or pigment and suspected to be TiO_2 , as suggested by the EDS shown in Additional file 1: Figure S2. The binder (un-regular shape of “white” to “glues” and connects particles together) will be tested below to confirm if or not they are plastic, and if or not the tiny

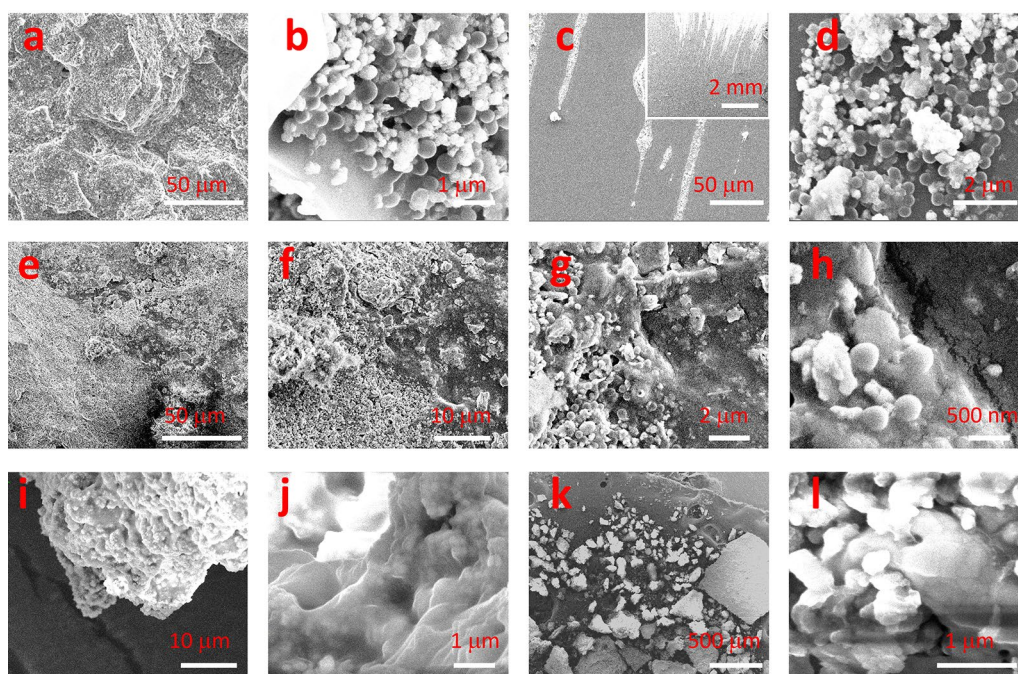


Fig. 1 SEM images. **a–d** Show the new paint on glass surface at different magnifications. **a, b** Are collected from the bulk paint surface and **c, d** from the branched paint surface. **e–h** Show the new paint (left-bottom part) on gyprock surface. **i, j** Are collected from the surface of a ~5-year-old paint peeled off from wood surface. **k, l** Are collected from the surface of a ~20-year-old paint peeled off from gyprock surface

structures in (b) are nanoplastics (being mixed with, coating and shelling the TiO₂ nanoparticles' surface).

In Fig. 1a, even the paint looks a bulk film, the film can be either broken (at the film boundary, or by friction, Additional file 1: Figure S1), or branched that originates from the painting process. In the latter case, the SEM images are shown in Fig. 1c, d. The detailed structure in (d) actually looks similar with that in (b), supporting the possibility to release micro-/nanoplastics/nanoparticles, if plastic is formulated in the paint.

The paint film on gyprock surface is presented in Fig. 1e–h. In (e), the left-bottom half is the painted area, which looks uniform and different from the right-top half where the gyprock surface is rough. Once zoomed in as (f, g), the paint film's boundary can release particles again. (h) shows that the TiO₂ nanoparticles are bounded by the binder again, either to coat the individual particle surface or to embed them as a bulk.

The similar structures are presented in Fig. 1i, j, which are collected from the peeled-off paint of ~5 years old. The bonded particles in (j) look similar with those in (b, d, h), although the binder or glue looks more, which depends on the paint quality and the painting process (e.g. multilayer coating vs. single layer coating, professional painting vs. DIY painting, etc.). For the paint of ~20 years old, the structures are presented in Fig. 1k, l. The zoomed in image in (l) looks similar with those in (b, d, h, j). The

peeled-off paint film is fragile and the fragments are presented in (k).

In most of cases, the individual particles can be observed, either on the paint film surface or at the boundary/edge/branch. In the following tests, we will characterise the plastics binder formulated in the paint. To simplify the characterisation, we focus on the fresh paint herein and test the old paint in Additional file 1.

Plastic identification

We selected several typical indoor paints (interior) for test in this study, as shown in Additional file 1: Figure S1. In order to avoid the interference originating from the colourful colourant, only native white paints are tested here. After painting and drying, Fig. 2a shows several typical spectra we collected. Given the complex formulation of the paint and the big family of acrylic polymer, we present the ABS spectrum (extracted from Rochman Lab) as reference in this study, to compare with the suspected acrylic binder in the paint. While the main peaks at ~1000 cm⁻¹ (C₆H), ~1230 cm⁻¹ (CO), ~1300 cm⁻¹ (CCO), ~1450 cm⁻¹ (CH), ~2910 cm⁻¹ (CH) and ~3050 cm⁻¹ (OH) (marked with dashed lines) appear to match with the styrene or acrylic [4, 32–34], the two broad/strong peaks at ~440 cm⁻¹ and ~610 cm⁻¹ (circulated) are assigned to the white colourant of TiO₂ [35].

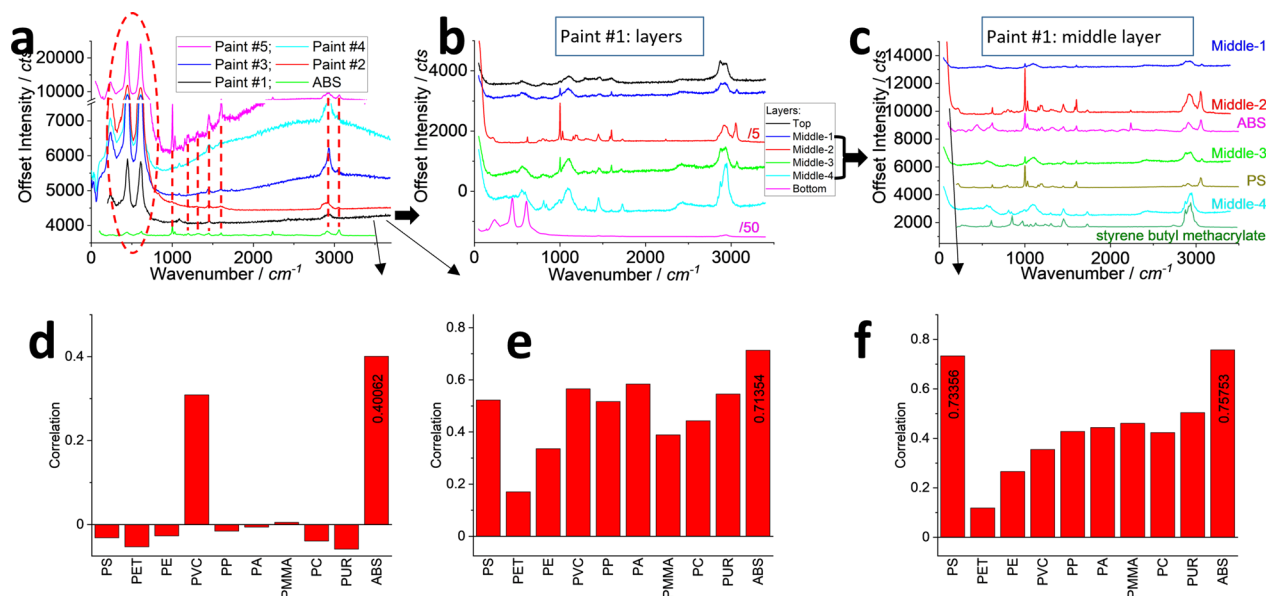


Fig. 2 Raman spectra (a–c) and correlation values (d–f) of the samples as indicated. All spectra intensities are off-set for presentation. The ABS spectrum is presented in a as reference to compare with different paints including #1–#5, according to the characteristic peaks marked with dashed lines, where the circled areas suggest the presence of TiO_2 . Sample #1 is centrifuged and separated to get layers that yield spectra in b. The middle layer is further analysed in c with the possible assignments as the references. In d–f, the spectra of paint sample #1 and its middle layer (Middle-2) are correlated with 10 common plastics including PS, PET, PE, PVC, PP, PA, PMMA, PC, PUR, and ABS, before (d, f) and after (e) removing the signal in the low wavenumber range [$<800\text{ cm}^{-1}$, circled in a] that is dominated by TiO_2

Although the main peaks are suspected to originate from styrene or acrylic, the exact component of plastics is not known. We thus treat and separate the liquid paint (before painting and drying) using centrifuge. We note there are roughly three layers, as shown in Additional file 1: Figure S1. The middle layer can be further separated as four layers using a high-speed centrifuge. From their spectra in Fig. 2(b), the top layer is the solvent and dominated by water, with some additives that are difficult to assign. They are also unstable under the laser because they can be easily burned by the Raman laser. The bottom layer is dominated by TiO_2 colourant. Its Raman activity is much higher than others because its intensity has been shrunken by 50 times. There are several sub-layers in the middle part and their spectra are also shown, which is further analysed in (c).

In Fig. 2c, at a different position of the middle layer, the spectrum is different. For example, the spectrum of Middle-1 is similar with the top layer, where the solvent and additives dominate the Raman scattering. The Middle-2 looks like ABS, particularly the peak at $\sim 2240\text{ cm}^{-1}$ can lead to this assignment. Middle-3 is close to PS due to the absence of the peaks at $\sim 2240\text{ cm}^{-1}$ and $\sim 1730\text{ cm}^{-1}$. Middle-4 is similar with the spectrum of a copolymer of styrene butyl methacrylate, which is also close to ABS but without the peak at $\sim 2240\text{ cm}^{-1}$. With these assignments, the paint/binder is a mixture, although the

different batch, colour, application and brand of paint can lead to the assignment variation. In this case, we can conclude that at least one of the main components is plastic that is used as the binder in the paints.

We can employ the correlation matrix to digitally justify and compare the target with 10 common plastics, the results are shown in Fig. 2d–f [31]. Taking the Paint #1 as an example, (d) indicates the assignment to ABS, if we take the highest correction value (~ 0.40062). This correlation value is low (far away from 1), mainly due to the interference from the TiO_2 . We can intentionally remove this low wavenumber range signal of interference ($<800\text{ cm}^{-1}$) and the correction value is then increased to ~ 0.71354 in (e). If we take the spectrum from the middle layer (after removing the co-components' interference), such as Middle-2 in Fig. 2c for the calculation, the correlation values can be further increased to ~ 0.75753 , suggesting the right direction to remove the interference towards identification. Due to the mixture of the paint and the similar spectra (such as with PS, because ABS' spectrum might also be dominated by PS, which depends on the copolymer component/ratio, curing process individually after separation or together without the separation, etc.), the second highest correction value is with PS at ~ 0.73356 . Again, we emphasise that this assignment just indicates the presence of main

“acrylic” in the tested paints, rather than the pure ABS because ABS is itself a family of polymers as well. More information is provided in Additional file 1: Figure S3.

For the old paints, the identification is more difficult than the fresh ones. The ageing leads to the decomposition of the plastics to some degree. At different positions and subject to different circumstances, the ageing-induced decomposition is different, as shown in Additional file 1: Figure S3. Particularly for a paint of ~20 years old, the identification gets more complicated, which is provided in Additional file 1: Figure S3 as well.

The SEM images in Fig. 1 and Raman identification in Fig. 2 suggest that there are plastic films formed from the dried/cured paints, by coating/bonding/embedding the nanoparticles. These plastic-coating/bonding/embedding nanoparticles of hybrid can be categorised as micro-/nanoplastics, depending on the size and the amount of plastic (such as mass percentage). In the following parts, we use a brush to distribute the paint on glass, gyprock, and wood surface, with some branched paint, as shown in Fig. 1c, d, and in Additional file 1: Figure S2, to capture the hybrid of plastic-coating/bonding/embedding nanoparticles at the boundary/edge of the paints. We also try to capture them on the bulk paint film surface (supported by Fig. 1a, b). However, the background from the bulk paint film is so high that the individual particles’ signal is masked, unless the individual particles (or aggregate) are well independent/pending from the bulk background (as shown in Fig. 6 below).

Paint#1 on glass surface

In this section, we test the paint branch deposited on the glass surface. The branches are observed in Fig. 3a. The typical spectra are presented in (b), to compare with a reference spectrum of ABS. Due to the shortened integration time of 1 s in Fig. 3b (vs. 10 s in Fig. 2), the spectra have the decreased signal–noise ratio.

However, the scan generates a hyper-spectrum matrix that contains 900 (30×30) spectra. By mapping the intensity from this matrix, the signal can be averaged and enhanced, from a statistical point of view. To validate this approach, we firstly map a blank wavenumber window where the paint has no signal. The generated image is shown in Fig. 3c. Only random noise is mapped, suggesting no signal from the paint in this area from this mapping window or channel.

We then map the two strong peaks at ~440 cm^{-1} and ~610 cm^{-1} . The generated images in Fig. 3d, e match well with that in (a) in most of areas, suggesting the presence of the TiO_2 colourant in the paint [35]. On the other hand, if the colourant and the plastic binder are well mixed together, we actually can employ this colourant as indicator to indicate the presence of the co-existed plastic. That is, images (d, e) can suggest not only the presence of TiO_2 directly, but also its co-existed plastic indirectly.

We also map the characteristic peaks of acrylic (using ABS as a reference) and generate images in Fig. 3f–j. Some images are clear in (h, i), some blurred in (f, j), and one not clear in (g). The reason beyond the paint mixture is due to the different peak intensity of acrylic, some

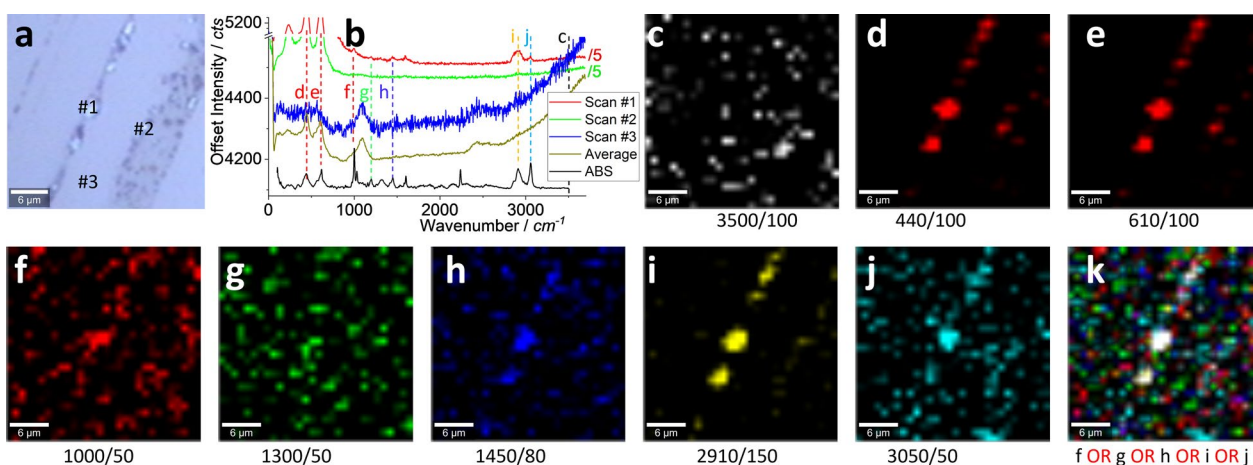


Fig. 3 Photo image (a), typical Raman spectra (b), and Raman intensity images (c–k) collected from the paint branches distributed on a glass surface. The area in a of 30 $\mu\text{m} \times 30 \mu\text{m}$ was scanned. Raman spectra were collected under an objective lens of 40 \times , integration time of 1 s for each pixel of 1 $\mu\text{m} \times 1 \mu\text{m}$ (to create a matrix of 30 \times 30). b Shows the Raman spectrum of ABS to compare with 3 typical spectra collected from the marked positions in a, and the averaged spectrum of 900 spectra (30 \times 30), with intensity off-setting for presentation. The intensity images (c–k) are mapped at a blank wavenumber window (c), two broad peaks (suspected colourant) (d, e), the characterised peaks of acrylic (f–j), and their merged one (using logic-OR) (k), as marked under each image (and the peak width) and in b, after 20% colour off-setting

peaks are intrinsically strong so that can generate a clean pattern with a higher signal–noise ratio than others. To cross-check them, we can merge all them together, to get image (k), using an algorithm of logic-OR. The white area thus contains the contributions from all those characteristic peaks, meaning an enhanced signal–noise ratio. The background (colourful dots) is mainly from images (f, g, j) where the characteristic peaks are not strong. Therefore, (k) can confirm and identify the present of plastic from the white area. After the assignment and confirmation, (i) can visualise it via the strongest peak, to yield a clearer background or a higher signal–noise ratio. In the following, we will focus the peak at $\sim 2910\text{ cm}^{-1}$ to visualise the acrylic-based plastic component in the paint.

Paint#1 on glass surface: high-resolution image of plastic-coating nanoparticles

To capture the possible hybrid microplastics and nanoplastics, we zoom in the scanning area and the results are presented in Fig. 4. Again, the photo image in (a) can indicate the presence of paint. The Raman spectra in (b) confirm this presence, from molecular spectrum point of view. Herein only the peak at $\sim 2910\text{ cm}^{-1}$ is strong, along with two broad peaks at $\sim 440\text{ cm}^{-1}$ and $\sim 610\text{ cm}^{-1}$ [35]. We thus map the strong peaks to generate images in (c, d). The pattern looks similar with slight difference, such

as at the central part pattern in (c) where two spots are comparable in size, while in (d) where the two spots are different in size. This difference is assigned to the different components/distributions in the paint. That is, (c) visualises the acrylic-based plastic while (d) the colourant.

We can merge them as Fig. 4e to compare them. The 3D version in (f) can highlight the difference more clearly. That is, different components in the paint can be individually visualised, a main advantage of the Raman imaging. The plastic-shelling/coating nanoparticles of TiO_2 can be clearly presented as a hybrid. More details are provided in Additional file 1: Figure S4.

Paint#2 on glass surface

Similarly, we test another paint sample (#2) and the results are shown in Fig. 5. Basically, the similar conclusion can be drawn, the mapped pattern of plastic in (d) matches well with (a), with colourant pattern in (e) that is slightly different from (d). However, some differences from above are also noted, the new image in (c) mapping a new peak at $\sim 1100\text{ cm}^{-1}$ in (b, arrowed) might be due to the new component in the paint, while other characteristic peaks of acrylic-based plastic are marked in (b) as well. Therefore, the new peak can be mapped as a new image that patterns differently from (d, e).

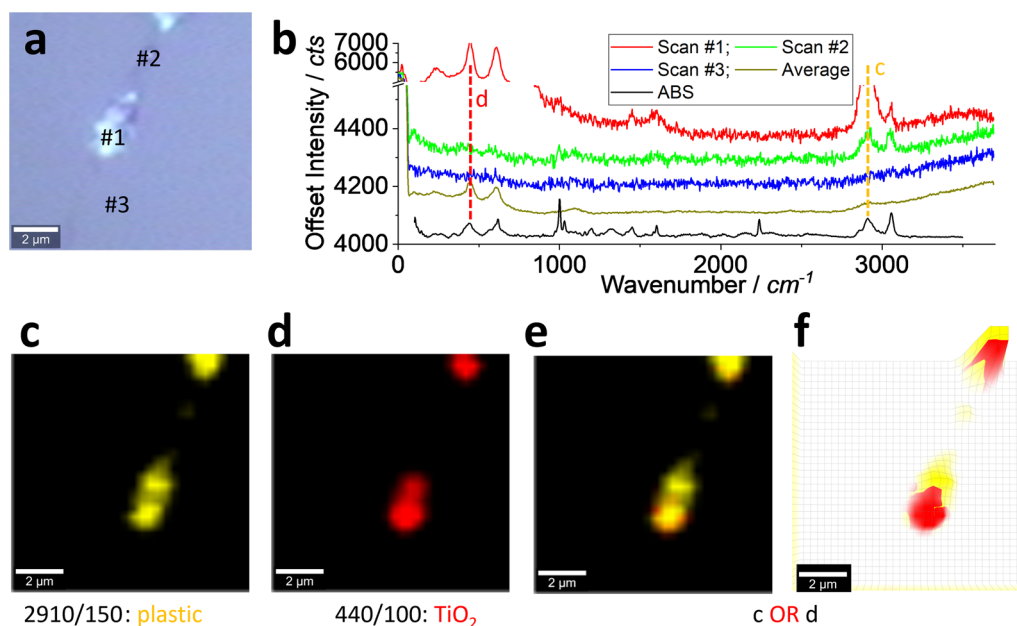


Fig. 4 Photo image (a), typical Raman spectra (b), and Raman intensity images (c–f) collected from the paint branches distributed on a glass surface. In a, the area of $10\text{ }\mu\text{m} \times 10\text{ }\mu\text{m}$ is scanned. Raman spectra were collected under an objective lens of 100 \times , integration time of 1 s for each pixel of $0.33\text{ }\mu\text{m} \times 0.33\text{ }\mu\text{m}$ (to create a spectrum matrix of 30×30). b Shows the Raman spectrum of ABS (with intensity off-setting for presentation), to compare with 3 typical spectra collected from the positions marked in a, and the scanning average spectrum. The intensity images (c–f) are mapped at the peak of acrylic at $\sim 2910\text{ cm}^{-1}$ (c) and colourant at $\sim 440\text{ cm}^{-1}$ (e), as marked under each image (and the peak width) and in b, after 20% colour off-setting. e Merges (c, d) using logic-OR. f Is another version of e, using 3D presentation and white background

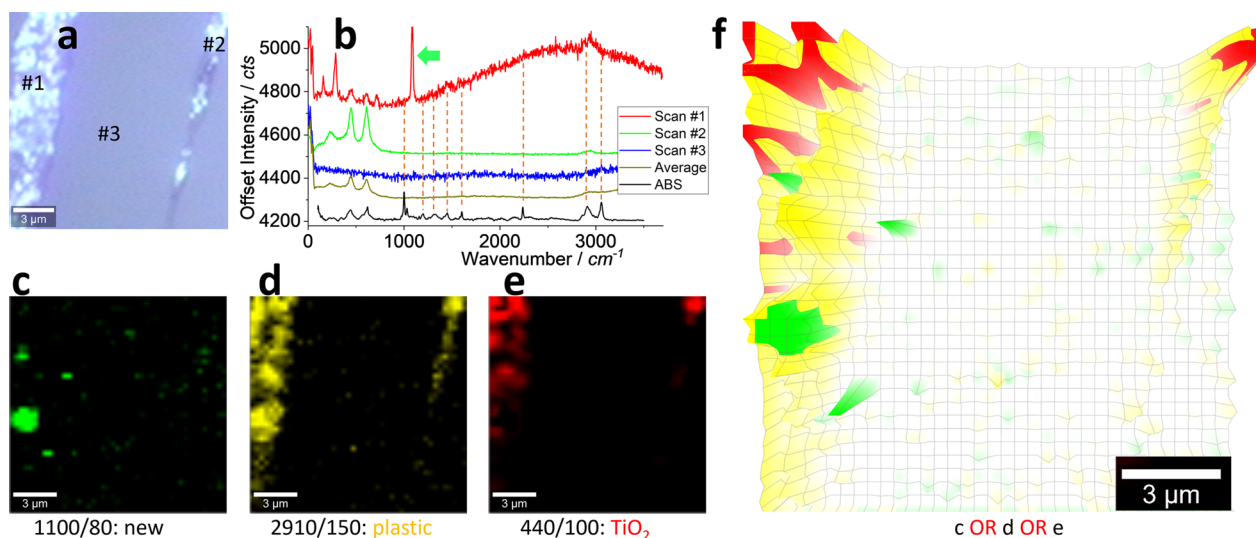


Fig. 5 Photo image (a), typical Raman spectra (b), and Raman intensity images (c–f) collected from the paint branches distributed on a glass surface. In a, the area of $15\ \mu\text{m} \times 15\ \mu\text{m}$ is scanned. Raman spectra were collected under an objective lens of 100 \times , integration time of 1 s for each pixel of $0.33\ \mu\text{m} \times 0.33\ \mu\text{m}$ (to create a spectrum matrix of 45×45). b Shows the Raman spectrum of ABS (with intensity off-setting for presentation), to compare with 3 typical spectra collected from the positions marked in a, and the scanning average spectrum. The intensity images (c–e) are mapped at a new peak one at $\sim 1100\ \text{cm}^{-1}$ (c), acrylic at $\sim 2910\ \text{cm}^{-1}$ (d) and colourant at $\sim 440\ \text{cm}^{-1}$ (e), as marked under each image (and the peak width), after 20% colour off-setting. f Merges (c–e), using 3D presentation and white background

We can merge them again in Fig. 5f, to visualise their different contributions in the same image. In the middle part, the patterned dots might be noise but need more research. In brief, the hybrid plastic-coating/embedding TiO_2 nanoparticles is confirmed again. More details are provided in Additional file 1: Figure S5.

Paint#2 on gyprock surface

Finally, we test the paint on gyprock that we generally use as the interior wall. The results are shown in Fig. 6. Although the gyprock yields a strong fluorescent background which complicates the analysis on plastic, the similar conclusion can be drawn again, including the mapped hybrid mixture of acrylic-based plastic and colourant in Fig. 6c. More information is provided in Additional file 1: Figure S6. Note herewith the hybrid mixture is well isolated/pending from the background bulk film on the gyprock surface, so that the signal can be effectively picked up by the confocal Raman.

To further increase the imaging signal–noise ratio by averaging the image background (not the spectrum background), we can re-construct the image in Fig. 6c via surface fitting [20–23]. Basically, the image is fitted to Gaussian surface towards deconvolution. The re-constructed images are compared with the original images in Fig. 6d, e, to visualise plastic and TiO_2 , respectively. From the contour lines of the re-constructed images, the surface fitting can effectively remove the background noise. Similarly, we can merge the re-constructed images (d, e)

as (f), to directly visualise the hybrid structure of plastic-coating/embedding TiO_2 nanoplastics again. Compared with image (c), image (f) after re-construction can have an increased assignment certainty.

More samples are tested and reported in Additional file 1: Figures S7–S9.

Health concern

Above tests and these in Additional file 1 can confirm the binder in the tested paints is plastic, although different paint might have different formulation. In Fig. 1, the SEM images of the paint suggest that the plastics components might release some small pieces or fragments, either at the boundary of paint film, at the broken films/branches, or at the peeled-off paint films, etc., which might be hybrid micro-/nanoplastics. During the painting process, the droplets released and observed in Additional file 1: Figure S1 can also be categorised as microplastics or nanoplastics, depending on the size. It is thus suggested that personal protective equipment (PPE) should be put on by the painters and we should be cautious for the aftermath clean-up.

Once cured and dried, the paint should be cautiously treated to avoid friction or broken, to minimise the possibility to release small pieces or fragments or debris, as shown in Additional file 1: Figure S1. Even so, the ageing and weathering of plastics, particularly for the indoor paint that we are exposed to every day, should be carefully studied towards risk assessment, as presented in

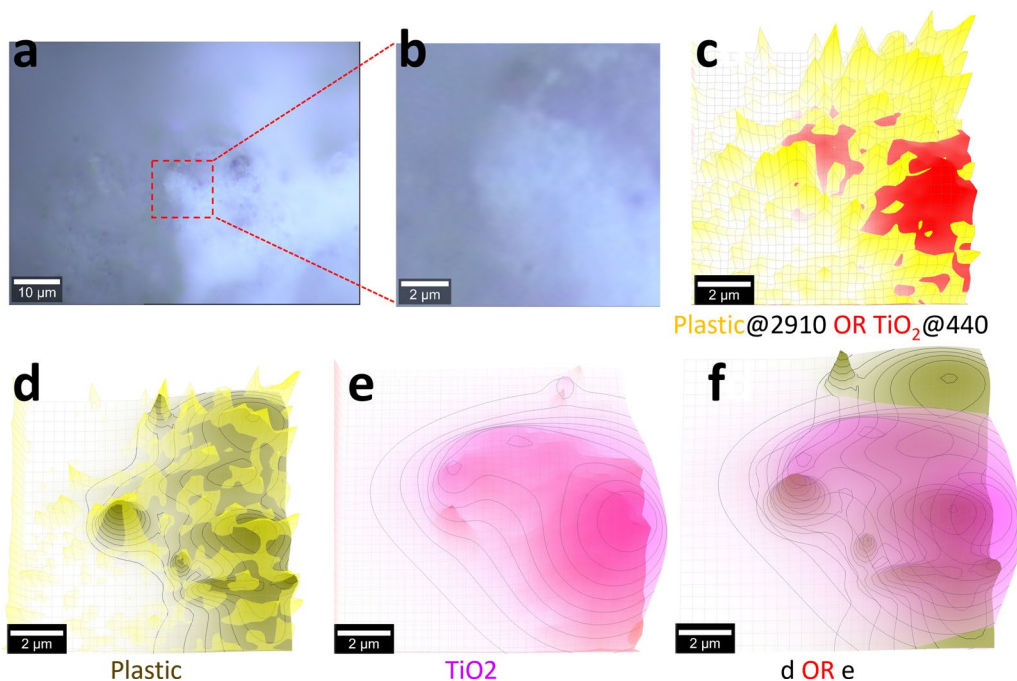


Fig. 6 Photo images (**a, b**) and Raman intensity images (**c–f**) collected from the paint distributed on a gyprock surface. In **a**, the squared area of $10\ \mu\text{m} \times 10\ \mu\text{m}$ is zoomed in as **b** and scanned. Raman spectra were collected under an objective lens of 100 \times , integration time of 1 s for each pixel of $0.33\ \mu\text{m} \times 0.33\ \mu\text{m}$ (to create a spectrum matrix of 30×30). The intensity image (**c**) map acrylic at $\sim 2910\ \text{cm}^{-1}$ (**d**) and colourant at $\sim 440\ \text{cm}^{-1}$ (**e**), respectively, as marked under the image, after 20% colour off-setting. **d, e** Re-construct (**c**) including mapping acrylic at $\sim 2910\ \text{cm}^{-1}$ (**d**) and colourant at $\sim 440\ \text{cm}^{-1}$ (**e**) using contour lines, respectively. **f** Merges (**d, e**) after re-construction

Additional file 1: Figures S7–S9. For example, whether or not this hybrid plastic-coating/embedding-nanoparticles differs from the pure micro-/nanoplastic and nanoparticles is an open question, in terms of risk assessment and fate [11, 12, 36, 37]. The similar hybrid structure of plastics-surrounding-sand has been reported before, but the risk assessment is absent too [18, 19].

The hybrid plastic-coating/embedding-nanoparticles can have a significant amount. For example, there are 50–100 hybrid particles in Fig. 1b, d in the typical area of $5\ \mu\text{m} \times 6\ \mu\text{m}$, which means an area of $1\ \text{cm} \times 1\ \text{cm}$ can contain ~ 170 – 340 millions of the hybrid particles. Considering the paint usually has a thickness of 100 – $200\ \mu\text{m}$ [5], while the thickness in Fig. 1b, d is $\sim 1\ \mu\text{m}$, an area of $1\ \text{cm} \times 1\ \text{cm}$ ($\times 100$ – $200\ \mu\text{m}$) can in total contain ~ 17 – 68 billions of the hybrid particles that are surrounding us daily. In other words, a house with $\sim 100\ \text{m}^2$ painted surface area might contain ~ 17 – 68 quadrillions (10^{15}) of the hybrid particles. Although most of them are painted as a bulk film as presented in Fig. 1, their fate such as being released into environment (in long term) is not clear so far, along with risk in potential [12, 36]. For example, whether or how the hybrid can be treated at the wastewater treatment plants is not clear, and the eventual situation at the landfill sites is not clear too. Given the

emerging concerns on the micro-/nanoplastics contamination, more research is needed [7, 37, 38].

The other released item (as vapours of benzene, toluene, ethylbenzene and xylene, or BTEX) is another concern, as presented in Additional file 1: Figure S10. The monitoring lasted for ~ 40 days. For the longer term of ageing (or degradation) process (~ 5 – 20 years, for example in this study), the BTEX monitoring is not available and beyond the scope of this research. It is suggested the risk assessment should be conducted, given that we are living in houses or offices that are generally painted.

Conclusion

We successfully characterise plastic from the paint mixture, along with the colourant of titanium dioxide, suggesting the advantage of Raman imaging. While the plastic debris release depends on a number of conditions, we should be cautious that we are surrounded by lots of plastic items in our daily lives that might release microplastics and even nanoplastics, gradually and secretly. As tested herein, most of the released items might be a mixture of colourant and plastic (such as plastic-coating/embedding TiO_2 nanoparticles), which is different from the pure plastic, the toxicity of this mixture or hybrid is

not yet known and needs assessment, given all of us are being exposed to the paints day and night.

There might be another debate on the hybrid of plastic-coating TiO₂ nanoparticles and plastic-embedding TiO₂ nanoparticles, can we categorise the hybrid nanoparticles as nanoplastics or not? The amount of plastic on the TiO₂ nanoparticles' surface (such as mass percentage) is unknown and the ageing/degradation of plastic in the presence of TiO₂ nanoparticles also needs more research. Perhaps the risk assessment can give us a clear information about this hybrid nanostructure, which is needed too.

Declaration of generative AI and AI-assisted technologies in the writing process

During the preparation of this work the author(s) used ChatGPT in order to write the introduction part. After using this tool/service, the author(s) reviewed and edited the content as needed and take(s) full responsibility for the content of the publication.

Supplementary Information

The online version contains supplementary material available at <https://doi.org/10.1186/s12302-024-00844-6>.

Additional file 1: Figure S1. Photo images. **Figure S2 & Table S1.** EDS & Raman parameters. **Figure S3.** Identification of plastics. **Figure S4.** More Raman images for Fig. 4. **Figure S5.** More Raman images for Fig. 5. **Figure S6.** More Raman images for Fig. 6. **Figure S7.** ~ 5-year-old paint (#5), peeled from a wood surface. **Figures S8–S9.** ~ 20-year-old paint (#6), peeled off from gyprock surface. **Figure S10.** release of BTEX.

Author contributions

CF, WZ, JH, CW wrote the main manuscript text after testing; JN, RN reviewed and managed the experiment. All authors reviewed the manuscript.

Funding

The authors appreciate the funding support from CRC CARE and the University of Newcastle, Australia. For the Raman measurements and SEM, we also acknowledge the use and support of the South Australian node of Microscopy Australia (formerly known as AMMRF) at Flinders University, South Australia.

Availability of data and materials

Data will be available on demand.

Declarations

Ethics approval and consent to participate

Not applicable.

Competing interests

The authors declare no competing interests.

Author details

¹Global Centre for Environmental Remediation (GCER), University of Newcastle, Callaghan, NSW 2308, Australia. ²CRC for Contamination Assessment and Remediation of the Environment (CRC CARE), University of Newcastle, Callaghan, NSW 2308, Australia. ³College of Chemistry and Materials, Jiangxi Agricultural University, Nanchang, Jiangxi 330045, China. ⁴School of Environmental Science & Engineering, Guangzhou University, Guangzhou 510206,

China. ⁵College of Environmental Science and Engineering, North China Electric Power University, Beijing 102206, China.

Received: 14 November 2023 Accepted: 14 January 2024

Published online: 22 January 2024

References

- FortuneBusinessInsights (2023) Paints and Coatings Market Size, Share & COVID-19 Impact Analysis, By Resin (Epoxy, Acrylic, Polyester, Alkyd, Polyurethane, and Others), By Technology (Waterborne, Solvent Borne, Powder Coating, and Others) By Application (Architectural, Automotive OEM, Marine, Coil, General Industries, Protective Coatings, Automotive Refinish, Industrial Wood, and Others), and Regional Forecast, 2023–2030. Paints and coatings market. P. Coatings. <https://www.fortunebusinessinsights.com/industry-reports/paints-and-coatings-market-101947>.
- Abdulsalam S, Maiwada ZD (2015) Production of emulsion house paint using polyvinyl acetate and gum Arabic as binder. *Int J Mater Sci Appl* 4:350
- Gelder JD, Vandenabeele P, Govaert F, Moens L (2005) Forensic analysis of automotive paints by Raman spectroscopy. *J Raman Spectrosc* 36(11):1059–1067
- Wiesinger R, Pagnin L, Anghelone M, Moretto LM, Orsega EF, Schreiner M (2018) Pigment and binder concentrations in modern paint samples determined by IR and Raman spectroscopy. *Angew Chem Int Ed* 57(25):7401–7407
- Lambourne R, Strivens TA (1999) Paint and surface coatings: theory and practice. Elsevier
- Elkins J (2019) What painting is. Routledge
- Filella M, Turner A (2023) Towards the global plastic treaty: a clue to the complexity of plastics in practice. *Environ Sci Eur* 35(1):99
- Hartmann NB, Hüffer T, Thompson RC, Hassellöv M, Verschoor A, Daugaard AE, Rist S, Karlsson T, Brennholt N, Cole M, Herrling MP, Hess MC, Ivleva NP, Lusher AL, Wagner M (2019) Are we speaking the same language? Recommendations for a definition and categorization framework for plastic debris. *Environ Sci Technol* 53(3):1039–1047
- Liao Z, Ji X, Ma Y, Lv B, Huang W, Zhu X, Fang M, Wang Q, Wang X, Dahlgren R, Shang X (2021) Airborne microplastics in indoor and outdoor environments of a coastal city in Eastern China. *J Hazard Mater* 417:126007
- Ivleva NP (2021) Chemical analysis of microplastics and nanoplastics: challenges, advanced methods, and perspectives. *Chem Rev* 121(19):11886–11936
- de Souza Machado AA, Ghadernezhad N, Wolinska J (2023) Potential for high toxicity of polystyrene nanoplastics to the European *Daphnia longispina*. *Environ Sci Eur* 35(1):78
- Gaylarde CC, Neto JAB, da Fonseca EM (2021) Paint fragments as polluting microplastics: a brief review. *Mar Pollut Bull* 162:111847
- Zhang J, Wang L, Kannan K (2020) Microplastics in house dust from 12 countries and associated human exposure. *Environ Int* 134:105314
- Mohamed Nor NH, Kooi M, Diepens NJ, Koelmans AA (2021) Lifetime accumulation of microplastic in children and adults. *Environ Sci Technol* 55(8):5084–5096
- Pletz M (2022) Ingested microplastics: do humans eat one credit card per week? *J Hazard Mater Lett* 3:100071
- Kooi M, Primpke S, Mintenig SM, Lorenz C, Gerdtz G, Koelmans AA (2021) Characterizing the multidimensionality of microplastics across environmental compartments. *Water Res* 202:117429
- Schwafert C, Sogne V, Welz R, Meier F, Klein T, Niessner R, Elsner M, Ivleva NP (2020) Nanoplastic analysis by online coupling of Raman microscopy and field-flow fractionation enabled by optical tweezers. *Anal Chem* 92:5813–5820
- Luo Y, Qi F, Gibson CT, Lei Y, Fang C (2022) Investigating kitchen sponge-derived microplastics and nanoplastics with Raman imaging and multivariate analysis. *Sci Total Environ* 824:153963
- Luo Y, Zhang X, Zhang Z, Naidu R, Fang C (2022) Dual-principal component analysis of the Raman spectrum matrix to automatically identify and visualize microplastics and nanoplastics. *Anal Chem* 94(7):3150–3157

20. Fang C, Luo Y, Chuah C, Naidu R (2023) Identification of microplastic fibres released from COVID-19 test swabs with Raman imaging. *Environ Sci Eur* 35(1):34
21. Fang C, Luo Y, Naidu R (2023) Microplastics and nanoplastics analysis: options, imaging, advancements and challenges. *TrAC, Trends Anal Chem* 166:117158
22. Fang C, Luo Y, Naidu R (2023) Super-resolution imaging of micro- and nanoplastics using confocal Raman with Gaussian surface fitting and deconvolution. *Talanta* 265:124886
23. Fang C, Luo Y, Naidu R (2023) Super-resolution Raman imaging towards visualisation of nanoplastics. *Anal Methods* 15(40):5300–5310
24. Khan MJ, Khan HS, Yousaf A, Khurshid K, Abbas A (2018) Modern trends in hyperspectral image analysis: a review. *Ieee Access* 6:14118–14129
25. Lu B, Dao PD, Liu J, He Y, Shang J (2020) Recent advances of hyperspectral imaging technology and applications in agriculture. *Remote Sensing* 12(16):2659
26. Paoletti M, Haut J, Plaza J, Plaza A (2019) Deep learning classifiers for hyperspectral imaging: a review. *ISPRS J Photogramm Remote Sens* 158:279–317
27. Dong M, Zhang Q, Xing X, Chen W, She Z, Luo Z (2020) A Raman database of microplastics weathered under natural environments. *Mendeley Data*. V2. <https://doi.org/10.17632/kpygrf9fg6.2>
28. Yunker PJ, Still T, Lohr MA, Yodh AG (2011) Suppression of the coffee-ring effect by shape-dependent capillary interactions. *Nature* 476:308
29. Sobhani Z, Al Amin M, Naidu R, Megharaj M, Fang C (2019) Identification and visualisation of microplastics by Raman mapping. *Anal Chim Acta* 1077:191–199
30. Li JF, Fan BT, Doucet J-P, Panaye A (2003) Spectral Code Index (SPECOIND): a general infrared spectral database search method. *Appl Spectrosc* 57(7):858–867
31. Fang C, Luo Y, Zhang X, Zhang H, Nolan A, Naidu R (2021) Identification and visualisation of microplastics via PCA to decode Raman spectrum matrix towards imaging. *Chemosphere* 286(Pt 2):131736
32. Brun N, Youssef I, Chevrel M-C, Chapron D, Schrauwen C, Hoppe S, Bourson P, Durand A (2013) In situ monitoring of styrene polymerization using Raman spectroscopy. Multi-scale approach of homogeneous and heterogeneous polymerization processes. *J Raman Spectrosc* 44(6):909–915
33. Dong J, Ozaki Y, Nakashima K (1997) Infrared, Raman, and near-infrared spectroscopic evidence for the coexistence of various hydrogen-bond forms in poly(acrylic acid). *Macromolecules* 30(4):1111–1117
34. Todica M, Stefan R, Pop C, Olar L (2015) IR and Raman investigation of some poly (acrylic) acid gels in aqueous and neutralized state. *Acta Phys Pol A* 128(1):128–135
35. Clegg IM, Everall NJ, King B, Melvin H, Norton C (2001) On-line analysis using Raman spectroscopy for process control during the manufacture of titanium dioxide. *Appl Spectrosc* 55(9):1138–1150
36. under Abrasion PN (2014) Evaluation of the Particle Aerosolization from n-TiO₂.
37. Warheit DB (2018) Hazard and risk assessment strategies for nanoparticle exposures: how far have we come in the past 10 years? *F1000Res* 7:376
38. Bressot C, Shandilya N, Nogueira ES, Cavaco-Paulo A, Morgeneyer M, Bihan OL, Aguerre-Chariol O (2015) Exposure assessment based recommendations to improve nanosafety at nanoliposome production sites. *J Nanomater* 2015:931405

Publisher's Note

Springer Nature remains neutral with regard to jurisdictional claims in published maps and institutional affiliations.